WM-05-115

arXiv:hep-ph/0507180v2 25 Jul 2005

Photoproduction of the Θ^+ resonance on the nucleon in a Regge model

H. Kwee

Department of Physics, College of William and Mary, Williamsburg, VA 23187, USA

M. Guidal

Institut de Physique Nucléaire Orsay, F-91406 Orsay, France

M.V. Polyakov

Institut für Theoretische Physik II,
Ruhr-Universität Bochum, D-44780 Bochum, Germany and
Petersburg Nuclear Physics Institute, 188350, Gatchina, Russia

M. Vanderhaeghen

Jefferson Laboratory, Newport News, VA 23606, USA and
Department of Physics, College of William and Mary, Williamsburg, VA 23187, USA

(Dated: 2nd February 2008)

Abstract

We estimate the reaction mechanisms for the photoproduction of the $\Theta^+(1540)$ resonance on the nucleon, through K and K^* Regge exchanges. We compare the size of the cross sections for the $\gamma n \to K^- \Theta^+$ and $\gamma p \to \bar{K}^0 \Theta^+$ reactions, and investigate their sensitivity to the spin-parity assignments $J^P = \frac{1}{2}^\pm, \frac{3}{2}^\pm$ for the Θ^+ resonance. The model allows to estimate the cross sections corresponding with a given upper bound on the width of the Θ^+. Within this model, the cross sections on the neutron are found to be around a factor 5 larger than the ones on the proton, due to the presence of charged K exchange for the reaction on a neutron target. Furthermore, the photon asymmetry is found to display a pronounced sensitivity to the parity of the Θ^+, making it a very promising observable to help determining the quantum numbers of the Θ^+ resonance.

PACS numbers: 13.60.Rj,13.60.Le,13.60.-r

I. INTRODUCTION

Since the announcement of the first claim of experimental evidence for the $S = 1$ baryon resonance by Spring 8 [1] which is well known as the Θ^+ today, there has been a great number of experiments reporting the observation of the Θ^+ [2, 3, 4, 5, 6, 7, 8, 9, 10]. These experiments represent a great variety of nuclear and particle physics experiments. The first experiment [1] is a photoproduction process on carbon nuclei. The subsequent experiments searched for the Θ^+ in photoproduction on the nucleon [3, 4, 5], electroproduction on the nucleon [6, 10], and using kaon beams [2], neutrino beams [7] and hadron beams [8, 9]. All of these experiments have some weaknesses which made any single claim for the Θ^+ not robust. If however taken together these experiments present significant claim for the Θ^+. Most of the criticism arises due to the low statistics of the data of most experiments, uncertainty in background estimates, specific angle cuts applied for the data analysis [2, 4, 5], mixed strangeness [6, 7, 8] and certain nuclear effect corrections [1, 3]. In addition there is also a claim of observation for $S = -2$ exotic pentaquarks [11], even though this claim cannot be reproduced [23, 24].

Criticism for the Θ^+ claim also arises because a fairly large number of experiments [12, 13, 14, 15, 16, 17, 18, 19, 20, 21, 22] did not find any evidence for the Θ^+. Most of these experiments are high energy-high statistics experiments and they can fall into two categories. The first category are the e^+e^- experiments [12, 13, 14, 15] and the second category are the hadron beam experiments [16, 17, 18, 19]. The e^+e^- experiments do not present credible challenge to the existence of the Θ^+ since it is very unlikely to produce the Θ^+ from these experiments. The hadron beam experiments present more serious rebuttal evidence to worry about, but like the e^+e^- experiments, without obvious production mechanism, the rebuttal is not very convincing. It is also important to point out that the SAPHIR result [4] has been ruled out by the recent CLAS g11 experiment [53]. Details of analysis for the positive results as well as the negative results for the pentaquark experiments can be found in [25].

From the theoretical point of view, QCD does not prohibit the existence of pentaquark states. If there are any prejudices, we should expect the existence of the exotic states such as dibaryons, dimesons, glueballs and pentaquarks. For the pentaquark, the problems are where to look for the states and how to distinguish them from the ordinary baryon resonances. Also if the states are very wide, the search might be futile since we will not be able to distinguish the resonances from the background. After years of searches with no results, the community seemed to give up when PDG after 1986 [26] dropped the section on searches for pentaquarks. Recent interest for pentaquarks was sparked again after the announcement from Spring 8 experiment [1]. The experiments were conducted with the guidance of the chiral quark soliton model estimate by Diakonov *et. al.* [27], which predicted the existence of a narrow baryon resonance with strangeness ($S = 1$) at mass around 1530 MeV. Critics for this paper can be found in [28, 29]. The paper also predicted that the resonance has spin 1/2 and positive parity as predicted by subsequent chiral soliton model works [30, 31, 32, 33]. A naive constituent quark model will give a negative parity state [34], even though it is also possible to have a positive parity state in a quark model if one introduces a P-wave in the spatial wavefunction [35, 36, 37]. As for the spin of the Θ^+, all theory paper to our knowledge predicts 1/2 and consider spin-3/2 to be a heavier excitation state, see *e.g.* Ref. [38].

The most puzzling issues from the theoretical point of view right now is the narrow width of the Θ^+. The chiral quark soliton model work by Diakonov *et. al* [27] did naturally predict an anomalously narrow width for the Θ^+. Some attempts also have been made in constituent quark models to explain the narrow width, *e.g.* [37, 39, 40]. For an early review on these theoretical issues see [41].

Clearly, to address the issues mentioned above, *i.e.* existence, spin-parity assignment and width of the pentaquark, more dedicated experiments are needed. Production mechanisms are a key aspect in this study since it has been argued that certain processes will not be effective to produce the pentaquark. Many efforts have been made in the past to study the θ^+ photo- and electroproduction processes [42, 43, 44, 45, 46, 47, 48, 49, 50, 51, 52], even though most of the cross section predictions have been ruled out by the recent JLAB g10 and g11 experiments [53, 54].

In this paper we make another effort to study the photoproduction mechanism for the Θ^+ using a Regge model, which has been found to successfully describe the main features of $K\Lambda$ and $K\Sigma$ photoproduction on the nucleon at *c.m.* energies above 2 GeV [56, 57]. In section II we discuss the theory of Regge exchange mechanism. We also discuss the relation of the width to the photoproduction cross section of the Θ^+. In view of upcoming high resolution experiments [55], such a link is needed to translate quantitatively an upper limit on the photoproduction cross section into an upper bound on the Θ^+ width. In section III we present the results of our calculation for the Θ^+ photoproduction cross sections. We also study photon asymmetry and decay angular distribution of the Θ^+ photoproduction. We close with our conclusion in section IV.

II. REGGE MODEL

At sufficiently high energies, above the nucleon resonance region, strangeness photo- and electroproduction reactions (e.g. $\gamma p \to K^+\Lambda, K^+\Sigma$) at forward angles are dominated by K and K^* Regge exchanges as has been proposed long time ago in Ref. [58], and studied in detail in view of numerous recent strangeness photo- and electroproduction data in Refs. [56, 57]. It was found in those works that the simple Regge model for open strangeness electromagnetic production reactions in terms of K and K^* exchanges provides an economical description and simple explanation of the forward angle data for total *c.m.* energy $W > 2$ GeV. It surprisingly reproduces the gross features of the data, even for $W < 2$ GeV, hinting that a sort of reggeon-resonance duality is at work.

In this work, our aim is to extend this model to the description of the process

$$\gamma(q) \, + \, N(p_N) \, \longrightarrow \, K(p_K) \, + \, \Theta^+(p_\Theta) \, . \tag{1}$$

The Mandelstam variables for this process are given by $s \equiv (p_N + q)^2$, $t \equiv (q - p_K)^2$, and $u \equiv (q - p_\Theta)^2$, satisfying $s + t + u = M_N^2 + m_K^2 + M_\Theta^2$, with M_N the nucleon mass, m_K the kaon mass, and M_Θ the mass of the Θ^+. In this work we take as value for the mass of the Θ^+ the value $M_\Theta = 1.54$ GeV, consistent with the experiments of Refs. [1, 2, 3, 4, 5, 6, 7, 8, 9]. Our description of the reaction (1) in terms of reggeized K and K^* t-channel exchanges is aimed at the region of large s ($W = \sqrt{s} > 2$ GeV) and small $-t$ ($-t << s$). We discuss subsequently the t-channel K and K^* Regge exchange processes for reaction (1) as is shown in Fig. 1.

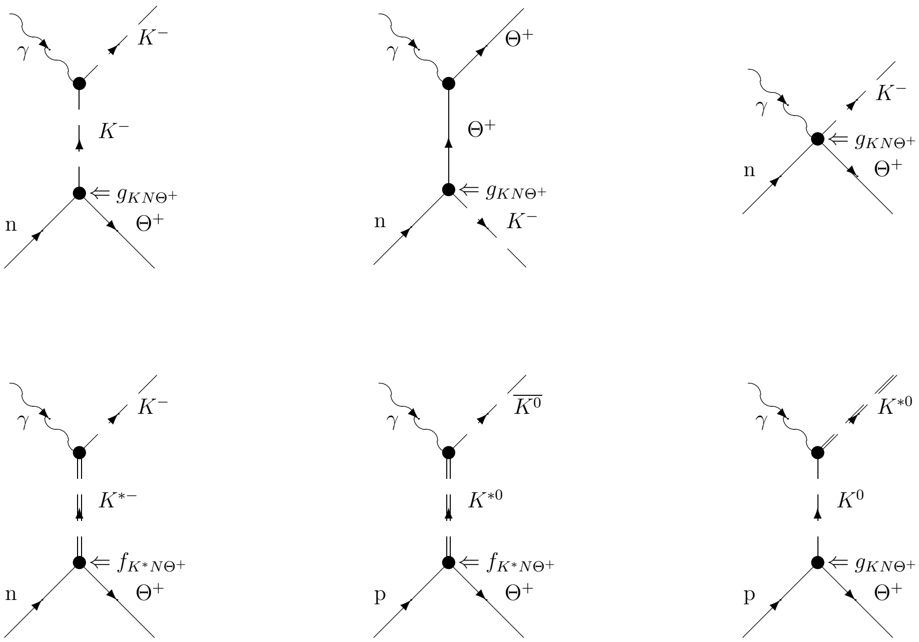

Figure 1: The different Regge exchange contributions considered to describe the photoproduction reactions with Θ^+ final state on a nucleon.

A. K Regge exchange

1. *Spin-1/2 Θ^+ Amplitude*

The construction of the reggeized amplitude for the charged K-exchange process to the $\gamma n \to K^- \Theta^+$ reaction, as shown in Fig. 1, amounts to replace the usual Feynman pole propagator for the kaon by a ‘Regge propagator' function, depending on both s and t, i.e. $\mathcal{P}^K_{Regge}(s,t)$ as follows :

$$\frac{1}{t-m_K^2} \Longrightarrow \mathcal{P}^K_{Regge}(s,t) \; = \; \left(\frac{s}{s_0}\right)^{\alpha_K(t)} \frac{\pi \alpha'_K}{\sin(\pi\alpha_K(t))} \, \frac{\mathcal{S}_K + e^{-i\pi\alpha_K(t)}}{2} \, \frac{1}{\Gamma(1+\alpha_K(t))} \, . \tag{2}$$

Such a Regge propagator function effectively takes into account the exchange of high-spin particles (in the t-channel) which lie on the K Regge trajectory $\alpha_K(t) = \alpha_K^0 + \alpha'_K \cdot t$. For the K, we use a standard linear trajectory in Eq. (2) :

$$\alpha_K(t) = 0.7\,(t - m_K^2) \; , \tag{3}$$

which was previously used in the analysis of strangeness photoproduction reactions at high energies [56]. Furthermore, in Eq. (2), the mass scale s_0 is typically taken as $s_0 = 1$ GeV^2, and $\mathcal{S} = \pm 1$ is the signature of the trajectory [59]. For the kaon trajectory, the states with $J^P = 0^-, 2^-, 4^-, ...$ correspond with $\mathcal{S} = +1$, whereas the states with $J^P = 1^+, 3^+, 5^+, ...$ correspond with $\mathcal{S} = -1$. The gamma function $\Gamma(1 + \alpha(t))$ suppresses poles of the propagator in the unphysical region. As is well known from Regge theory [59], trajectories can be either non-degenerate or degenerate. A degenerate trajectory is obtained by adding or subtracting the two non-degenerate trajectories with the two opposite signatures. As can be seen from the numerator of Eq. (2), this leads to trajectories with either a rotating ($e^{-i\pi\alpha(t)}$) or a constant (1) phase. In line with the finding of Ref. [56] for the charged K trajectory entering in strangeness photoproduction processes, we use the rotating phase in the following. This corresponds with the so-called strong degeneracy assumption [59] in Regge terminology, and amounts to replace in Eq. (2) the factor $(\mathcal{S}_K + e^{-i\pi\alpha_K(t)})/2$ by $e^{-i\pi\alpha_K(t)}$. One can easily verify that the Regge propagator reduces to the Feynman propagator $1/(t - m_K^2)$ if one approaches the first pole on a trajectory (i.e. when taking $t \to m_K^2$ in Eq. (2)).

In order to calculate the K Regge exchange contribution to the Θ^+ photoproduction amplitude as shown in Fig. 1, we have to specify the $KN\Theta^+$ vertex function. We subsequently study this vertex for the cases of spin and parity assignments $1/2^\pm$ and $3/2^\pm$ of the Θ^+ resonance.

- $J^P = \frac{1}{2}^+$

  For the spin parity assignment of the Θ^+ resonance given by $J^P = \frac{1}{2}^+$, the $KN\Theta^+$ vertex can be written as :

$$\mathcal{L}_{KN\Theta} = i\, g_{KN\Theta} \left(K^\dagger \bar{\Theta} \gamma_5 N + \bar{N} \gamma_5 \Theta K \right) , \tag{4}$$

  where K and N are the kaon and nucleon isospin doublet fields respectively, and where Θ is the Θ^+ isosinglet field. The Lagrangian of Eq. (4) corresponds with the Θ^+ being a p-wave resonance in the KN system. With this Lagrangian, the decay width $\Gamma_{\Theta \to KN}$ is given by :

$$\Gamma_{\Theta \to KN} = \frac{g_{KN\Theta}^2}{2\pi} \frac{|\bar{p}_K|}{M_\Theta} \left(\sqrt{\bar{p}_K^2 + M_N^2} - M_N \right) , \tag{5}$$

where $|\bar{p}_K| \simeq 0.267$ GeV is the kaon momentum in the rest frame of the Θ^+. To extract a value for $g_{KN\Theta}$, we need the experimental information of the width $\Gamma_{\Theta \to KN}$, which is not known precisely at this moment but whose measurement is the subject of several planned dedicated experiments, e.g. Refs.[55]. To provide numerical estimates in this work, we will use $\Gamma_{\Theta \to KN} = 1$ MeV as the value for the width, which is consistent with the upper limit for the width derived from elastic KN scattering [60]. Evaluating Eq. (5) with $\Gamma_{\Theta \to KN} = 1$ MeV, we then extract the value $g_{KN\Theta} \simeq 1.056$, which will be used in all of the following estimates for $J^P = \frac{1}{2}^+$ Θ^+.

- $J^P = \frac{1}{2}^-$
  For the spin parity assignment of the Θ^+ resonance given by $J^P = \frac{1}{2}^-$, the $KN\Theta^+$ vertex can be written as :

  $$\mathcal{L}_{KN\Theta} = g_{KN\Theta} \left(K^\dagger \bar{\Theta} N + \bar{N} \Theta K \right) , \tag{6}$$

  which corresponds with the Θ^+ being a s-wave resonance in the KN system. In this case, the decay width $\Gamma_{\Theta \to KN}$ is given by :

  $$\Gamma_{\Theta \to KN} = \frac{g^2_{KN\Theta}}{2\pi} \frac{|\bar{p}_K|}{M_\Theta} \left(\sqrt{\bar{p}_K^2 + M_N^2} + M_N \right) . \tag{7}$$

  Using $\Gamma_{\Theta \to KN} = 1$ MeV as the value for the width, we obtain $g_{KN\Theta} \simeq 0.1406$, which will be used in the following estimates for $J^P = \frac{1}{2}^-$ Θ^+.

Having specified the Regge propagator and $KN\Theta$ vertex function, we can construct the gauge invariant reggeized charged K-exchange amplitude for the $\gamma n \to K^- \Theta^+$ process for the spin-1/2 Θ^+ as :

$$\begin{aligned}
\mathcal{M}_K \left(\gamma n \to K^- \Theta^+ : J^P_\Theta = \frac{1}{2}^+ \right) \;&=\; e\, g_{KN\Theta} \cdot \mathcal{P}^K_{Regge}(s,t) \cdot \varepsilon_\mu(q,\lambda) \\
&\times\; \Big[F_K(t) \cdot (2p_K - q)^\mu \cdot \bar{\Theta}\, \gamma^5\, N \\
&-\; F_\Theta(u) \cdot (t - m_K^2) \cdot \bar{\Theta}\, \gamma^\mu \frac{(\gamma \cdot p_u + M_\Theta)}{u - M_\Theta^2} \gamma^5\, N \\
&+\; 2p_K^\mu \cdot (\hat{F}(s,t,u) - F_K(t)) \cdot \bar{\Theta}\, \gamma^5\, N
\end{aligned}$$

$$- \left(\frac{t - m_K^2}{u - m_\Theta^2} \right) \cdot 2p_\Theta^\mu \cdot \{\hat{F}(s,t,u) - F_\Theta(u)\} \cdot \bar{\Theta}\, \gamma^5 \, N \Bigg] \, , \tag{8}$$

$$\begin{aligned} \mathcal{M}_K \left(\gamma n \to K^- \Theta^+ : J_\Theta^P = \frac{1}{2}^- \right) &= (-i)\, e\, g_{KN\Theta} \cdot \mathcal{P}^K_{Regge}(s,t) \cdot \varepsilon_\mu(q,\lambda) \\ &\times \Big[F_K(t) \cdot (2p_K - q)^\mu \cdot \bar{\Theta}\, N \\ &- F_\Theta(u) \cdot (t - m_K^2) \cdot \bar{\Theta}\, \gamma^\mu \frac{(\gamma \cdot p_u + M_\Theta)}{u - M_\Theta^2} N \\ &+ 2p_K^\mu \cdot (\hat{F}(s,t,u) - F_K(t)) \cdot \bar{\Theta}\, N \\ &- \left(\frac{t - m_K^2}{u - m_\Theta^2} \right) \cdot 2p_\Theta^\mu \cdot \{\hat{F}(s,t,u) - F_\Theta(u)\} \cdot \bar{\Theta}\, N \Big] \, , \end{aligned} \tag{9}$$

where $\varepsilon_\mu(q,\lambda)$ is the photon polarization vector with photon polarization $\lambda = \pm 1$. To evaluate the Regge vertex functions (Regge residues) away from the pole position, we include the form factors $F_K(t)$, $F_\Theta(u)$, and $\hat{F}$ in the amplitude formulas above. In our calculations, we choose monopole forms for F_K and F_u :

$$F_K(t) = \left(1 + \frac{-t + m_K^2}{\Lambda^2} \right)^{-1} , \tag{10}$$

$$F_\Theta(u) = \left(1 + \frac{-u + M_\Theta^2}{\Lambda^2} \right)^{-1} . \tag{11}$$

For the cut-off Λ, we choose a typical hadronic scale of $\Lambda = 1$ GeV. In Eqs. (8,9), the terms proportional to F_K are the t-channel process (top left diagram in Fig. 1), whereas the terms proportional to F_u originate from the process with the Θ^+ in the u-channel (top middle diagram in Fig. 1). In the Regge approach, this gauge restoring term is reggeized in the same way as for the t-channel process, see e.g. Refs. [56, 61]. In particular, one notices that at the K pole, the pre-factors $(t - m_K^2)$ in the second terms of Eqs. (8,9) exactly compensate the Regge function $\mathcal{P}^K_{Regge}$, reducing these contributions to standard u-channel pole terms. For the $\gamma p \to K^+(\Lambda, \Sigma)$ reactions, it has been shown in Ref. [57] that this gauge invariant reggeization procedure (for the case where the form factors are absent), by restoring the gauge invariance of the t-channel charged kaon exchange process through proper reggeization of the s-channel (for K^+) or u-channel (for K^-) processes, is a key to reproduce several strangeness photo- and electroproduction observables. The third and fourth terms which contain $\hat{F}$ are contact terms which are required by gauge invariance when including form factors. The only restriction we applied to these terms is they should not have poles at $t = m_K^2$ and $u = m_\Theta^2$. With this restriction, we can choose the form :

$$\hat{F}(s,t,u) = F_K(t) + F_\Theta(u) - F_K(t) \cdot F_\Theta(u). \tag{12}$$

Note that $\hat{F} - F_K(t)$ is proportional to $(t - m_K^2)$, whereas $\hat{F} - F_\Theta(u)$ is proportional to $(u - M_\Theta^2)$, thus canceling the poles in the contact terms.

2. *Spin-3/2 Θ^+ Amplitude*

- $J^P = \frac{3}{2}^+$

  For the spin parity assignment of the Θ^+ resonance given by $J^P = \frac{3}{2}^+$, the $KN\Theta^+$ vertex can be written as :

  $$\mathcal{L}_{KN\Theta} = \frac{g_{KN\Theta}}{m_K} \left\{ \bar{\Theta}^\alpha g_{\alpha\beta} N \left(\partial^\beta K\right) + \bar{N} \Theta^\alpha g_{\alpha\beta} \left(\partial^\beta K^\dagger\right) \right\} .$$

  The Lagrangian of Eq. (13) corresponds with the Θ^+ being a p-wave resonance in the KN system. In this case, the decay width $\Gamma_{\Theta\to KN}$ is given by :

  $$\Gamma_{\Theta\to KN} = \frac{g_{KN\Theta}^2}{2\pi} \frac{|\bar{p}_K|}{M_\Theta} \frac{|\bar{p}_K|^2}{3m_K^2} \left(\sqrt{\bar{p}_K^2 + M_N^2} + M_N \right) .$$

  Again using $\Gamma_{\Theta\to KN} = 1$ MeV as value for the width, we obtain $g_{KN\Theta} \simeq 0.4741$, which will be used in the following estimates for $J^P = \frac{3}{2}^+$ Θ^+.

- $J^P = \frac{3}{2}^-$

  For the spin parity assignment of the Θ^+ resonance given by $J^P = \frac{3}{2}^-$, the $KN\Theta^+$ vertex can be written as :

  $$\mathcal{L}_{KN\Theta} = \frac{g_{KN\Theta}}{m_K} \left\{ \bar{\Theta}^\alpha \gamma_5 N g_{\alpha\beta} \left(\partial^\beta K\right) + \bar{N} \gamma_5 \Theta^\alpha g_{\alpha\beta} \left(\partial^\beta K^\dagger\right) \right\} .$$

  The Lagrangian of Eq. (13) corresponds with the Θ^+ being a d-wave resonance in the

KN system. In this case, the decay width $\Gamma_{\Theta\to KN}$ is given by :

$$\Gamma_{\Theta\to KN} \;=\; \frac{g^2_{KN\Theta}}{2\pi}\,\frac{|\bar{p}_K|}{M_\Theta}\,\frac{|\bar{p}_K|^2}{3m_K^2}\left(\sqrt{\bar{p}_K^2+M_N^2}-M_N\right).$$

Finally, using $\Gamma_{\Theta\to KN}=1$ MeV as value for the width, we obtain $g_{KN\Theta}\simeq 3.558$, which will be used in the following estimates for $J^P=\frac{3}{2}^-\ \Theta^+$.

Having specified the $KN\Theta$ vertex function for spin-3/2, we can construct the gauge invariant reggeized charged K-exchange amplitude for the $\gamma n\to K^-\Theta^+$ process for the $3/2^-\ \Theta^+$ as :

$$\begin{aligned}
\mathcal{M}_K\left(\gamma n\to K^-\Theta^+ : J^P_\Theta=\frac{3}{2}^+\right) \;=\;& \frac{i\,e\,g_{KN\Theta}}{m_K}\cdot\mathcal{P}^K_{Regge}(s,t)\cdot\varepsilon_\mu(q,\lambda)\\
\times\;& \Big[F_K(t)\cdot(2p_K-q)^\mu\cdot(p_K-q)^\alpha\cdot\bar{\Theta}_\alpha\,N\\
-\;& F_\Theta(u)\cdot(t-m_K^2)\cdot\bar{\Theta}_\alpha\,\gamma^{\alpha\beta\mu}\frac{(\gamma\cdot p_u+M_\Theta)}{u-M_\Theta^2}\\
&\qquad\cdot S_{\beta\nu}\cdot\gamma^{\nu\sigma\rho}\frac{(p_K)_\sigma\cdot(p_u)_\rho}{M_\Theta^2}N\\
+\;& (t-m_K^2)\cdot\bar{\Theta}_\alpha\,\gamma^{\alpha\mu\nu}\frac{(F_\Theta(u)\cdot p_K+F_K(t)\cdot p_\Theta)_\nu}{M_\Theta}N\\
+\;& 2p_K^\mu\cdot(\hat{F}(s,t,u)-F_K(t))\cdot p_K^\alpha\cdot\bar{\Theta}\,N\\
-\;& \left(\frac{t-m_K^2}{u-m_\Theta^2}\right)\cdot 2p_\Theta^\mu\cdot\{\hat{F}(s,t,u)-F_\Theta(u)\}\cdot p_K^\alpha\cdot\bar{\Theta}\,N\Big],
\end{aligned}\tag{13}$$

$$\begin{aligned}
\mathcal{M}_K\left(\gamma n\to K^-\Theta^+ : J^P_\Theta=\frac{3}{2}^-\right) \;=\;& \frac{-e\,g_{KN\Theta}}{m_K}\cdot\mathcal{P}^K_{Regge}(s,t)\cdot\varepsilon_\mu(q,\lambda)\\
\times\;& \Big[F_K(t)\cdot(2p_K-q)^\mu\cdot(p_K-q)^\alpha\cdot\bar{\Theta}_\alpha\,\gamma^5\,N\\
-\;& F_\Theta(u)\cdot(t-m_K^2)\cdot\bar{\Theta}_\alpha\,\gamma^{\alpha\beta\mu}\frac{(\gamma\cdot p_u+M_\Theta)}{u-M_\Theta^2}\\
&\qquad\cdot S_{\beta\nu}\cdot\gamma^{\nu\sigma\rho}\frac{(p_K)_\sigma\cdot(p_u)_\rho}{M_\Theta^2}\gamma^5 N\\
+\;& (t-m_K^2)\cdot\bar{\Theta}_\alpha\,\gamma^{\alpha\mu\nu}\frac{(F_\Theta(u)\cdot p_K+F_K(t)\cdot p_\Theta)_\nu}{M_\Theta}\gamma^5 N\\
+\;& 2p_K^\mu\cdot(\hat{F}(s,t,u)-F_K(t))\cdot p_K^\alpha\cdot\bar{\Theta}\,\gamma^5\,N
\end{aligned}$$

$$- \left(\frac{t - m_K^2}{u - m_\Theta^2}\right) \cdot 2p_\Theta^\mu \cdot \{\hat{F}(s,t,u) - F_\Theta(u)\} \cdot p_K^\alpha \cdot \bar{\Theta}\,\gamma^5\,N\Bigg] \,, \tag{14}$$

with

$$S_{\beta\nu} = g_{\beta\nu} - \frac{\gamma_\beta\,\gamma_\nu}{3} - \frac{(\gamma_\beta\,(p_u)_\nu - \gamma_\nu\,(p_u)_\beta)}{3M_\Theta} - \frac{2\,((p_u)_\beta(p_u)_\nu)}{3M_\Theta} \,.$$

Similar to the spin-1/2 case, the form factors $F_K(t)$ and $F_\Theta(u)$ have to be added to take into account the change of coupling constant $g_{KN\Theta}$ away from the pole position. In the calculation, we choose the same forms of $F_K(t)$ and $F_\Theta(u)$ for spin-3/2 as for the spin-1/2 case. For the spin-3/2 case we have to add the third, fourth and fifth terms in Eqs. (13,14), which originate from the contact diagrams to the t- and u-channel process to preserve gauge invariant in the amplitude. In the Regge approach, this gauge restoring term is reggeized in the same way as for the t-channel process, as discussed before for the spin-1/2 case. We also choose the $\hat{F}(s,t,u)$ to have the same form as for the spin-1/2 case.

B. K^* Regge exchange

We next consider the $K^*(892)$ exchange processes to both the $\gamma n \to K^-\Theta^+$ and $\gamma p \to \bar{K}^0\Theta^+$ reactions as shown in Fig. 1. Note that for the $\gamma p \to \bar{K}^0\Theta^+$ reaction, K exchange is not possible as the real photon does not couple to the neutral kaon. Therefore, we expect K^* exchange to be the dominant t-channel mechanism for the $\gamma p \to \bar{K}^0\Theta^+$ reaction.

The construction of the reggeized amplitude for the K^*-exchange processes, amounts to replace the K^* pole by a 'Regge propagator' function $\mathcal{P}_{Regge}^{K^*}(s,t)$:

$$\frac{1}{t - m_{K^*}^2} \Longrightarrow \mathcal{P}_{Regge}^{K^*} = \left(\frac{s}{s_0}\right)^{\alpha_{K^*}(t)-1} \frac{\pi\alpha'_{K^*}}{\sin(\pi\alpha_{K^*}(t))} \, \frac{\mathcal{S}_K^* + e^{-i\pi\alpha_{K^*}(t)}}{2} \, \frac{1}{\Gamma(\alpha_{K^*}(t))} \,, \tag{15}$$

For the $K^*(892)$, we use a standard linear trajectory :

$$\alpha_{K^*}(t) = 0.25 + \alpha'_{K^*}\,t \,, \tag{16}$$

where $\alpha'_{K^*} = 0.83$ GeV^{-2}. Furthermore, we also consider a degenerate trajectory for K^* leading to a Regge propagator with rotating phase in Eq. (15), in line with our previous findings in the analysis of strangeness photoproduction reactions at high energies [56].

To evaluate the K^* processes in Fig. 1, we next have to specify the $K^*N\Theta^+$ vertex function. If the spin parity assignment of the Θ^+ resonance is given by $J^P = \frac{1}{2}^+$, the $K^*N\Theta^+$ vertex can be written as :

$$\mathcal{L}_{K^*N\Theta} = f_{K^*N\Theta}\, \bar{\Theta} \left[\frac{i\,\sigma_{\mu\nu}\, p^{\nu}_{K^*}}{M_N + M_\Theta}\right] N \cdot V^{\mu}(p_{K^*}) + \text{h.c.}\,, \tag{17}$$

where $V^{\mu}(p_{K^*})$ is the polarization vector of the K^* meson. If the spin parity assignment of the Θ^+ resonance is given by $J^P = \frac{1}{2}^-$, the $K^*N\Theta^+$ vertex is given by :

$$\mathcal{L}_{K^*N\Theta} = -i\, f_{K^*N\Theta}\, \bar{\Theta} \left[\frac{i\,\sigma_{\mu\nu}\, p^{\nu}_{K^*}}{M_N + M_\Theta}\right] \gamma_5\, N \cdot V^{\mu}(p_{K^*}) + \text{h.c.}\,. \tag{18}$$

Using $SU(3)$ symmetry for the vector meson couplings within the baryon octet and between the baryon octet and antidecuplet, one can express :

$$\begin{aligned}
g_{\rho^0 pp} + f_{\rho^0 pp} &= \frac{7}{10}\left(V_0 + \frac{1}{2}V_1\right) + \frac{1}{20}V_2, & (19)\\
g_{\omega pp} + f_{\omega pp} &= \frac{1}{10}\left(V_0 + \frac{1}{2}V_1\right) + \frac{23}{20}V_2, & (20)\\
g_{\phi pp} + f_{\phi pp} &= -\frac{1}{10}\left(V_0 + \frac{1}{2}V_1\right) + \frac{7}{20}V_2, & (21)\\
f_{K^{*0}\Theta^+ p} &= \frac{3}{\sqrt{30}}\left(V_0 - V_1 - \frac{1}{2}V_2\right), & (22)
\end{aligned}$$

where $g_{VNN}(f_{VNN})$ are the vector (tensor) coupling constants respectively. First we use the fact that $g_{\phi pp} + f_{\phi pp} \simeq 0$ [62], and solve for V$_2$ in Eq. (21). Substituting this into Eqs. (19) and (22), we can express the $K^*N\Theta$ coupling as :

$$f_{K^{*0}p\Theta^+} = (g_{\rho^0 pp} + f_{\rho^0 pp})\,\frac{3\sqrt{3}}{\sqrt{10}}\,\frac{4/5 - r}{r + 2}\,, \tag{23}$$

where r is defined as $r \equiv V_1/V_0$. By fixing the ratio r to its value obtained in the chiral quark soliton model [27] : $r \simeq 0.35$ and using the value $g_{\rho^0 pp} + f_{\rho^0 pp} \simeq 18.7$ [63], Eq. (23) then leads to the coupling $f_{K^*N\Theta} = \simeq 5.9$. Note that the value of $f_{K^{*0}p\Theta^+}$ is very sensitive to the value of the parameter r, as there is a strong cancellation of various contributions.

The case of 1 MeV width of Θ^+ indicates that this cancellation can be very deep. The above mentioned value obtained in the particular dynamical model is subjected to large theoretical uncertainties which result in big spread in values of the coupling constant. Here we assume that the parameter r is close to the value of its counterpart for the axial transitions which corresponds with a width of Θ^+ of about 1 MeV. This assumption yields :

$$f_{K^* N\Theta} \equiv f_{K^{*0} p\Theta^+} \simeq 1.1 \,, \tag{24}$$

which will be used for the coupling constant entering in the vertices of Eqs. (17,18) for both parities of the Θ^+.

The reggeized K^* exchange amplitudes for both parities of the Θ^+ are then given by :

$$\begin{aligned}
\mathcal{M}_{K^*}\left(\gamma p \to \bar{K}^0\Theta^+ : J^P_\Theta = \frac{1}{2}^+\right) &= i\, e\, f_{K^{*0}K^0\gamma}\; f_{K^*N\Theta} \cdot \mathcal{P}^{K^*}_{Regge}(s,t) \cdot \varepsilon^\mu(q,\lambda) \\
&\times\; \varepsilon_{\mu\nu\lambda\alpha}\, q^\nu\, (q-p_K)^\lambda\, \bar{\Theta} \left[\frac{i\,\sigma^{\alpha\beta}\,(q-p_K)_\beta}{M_N + M_\Theta} \right] N \,, \qquad (25) \\
\mathcal{M}_{K^*}\left(\gamma p \to \bar{K}^0\Theta^+ : J^P_\Theta = \frac{1}{2}^-\right) &= e\, f_{K^{*0}K^0\gamma}\; f_{K^*N\Theta} \cdot \mathcal{P}^{K^*}_{Regge}(s,t) \cdot \varepsilon^\mu(q,\lambda) \\
&\times\; \varepsilon_{\mu\nu\lambda\alpha}\, q^\nu\, (q-p_K)^\lambda\, \bar{\Theta} \left[\frac{i\,\sigma^{\alpha\beta}\,(q-p_K)_\beta}{M_N + M_\Theta} \right] \gamma_5\, N \,, \qquad (26)
\end{aligned}$$

and analogous formulas hold for the K^* contribution to the $\gamma n \to K^-\Theta^+$ reaction. In Eqs. (25,26), the electromagnetic coupling $f_{K^*K\gamma}$ can be extracted from the radiative decay widths $\Gamma_{K^{*0}\to K^0\gamma} = 0.117$ MeV, and $\Gamma_{K^{*-}\to K^-\gamma} = 0.05$ MeV, yielding [56] :

$$\begin{aligned}
f_{K^{*0}K^0\gamma} &= 1.28 \;\; \mathrm{GeV}^{-1} \,, \qquad (27) \\
f_{K^{*-}K^-\gamma} &= 0.84 \;\; \mathrm{GeV}^{-1} \,. \qquad (28)
\end{aligned}$$

Note that the K^* t-channel exchange amplitudes of Eqs. (25,26) are gauge invariant by themselves.

III. RESULTS

In Fig. 2, we show our results for the differential cross section for the $\gamma n \to K^-\Theta^+$ reaction for the cases of spin-parity assignments $1/2^\pm$ and $3/2^\pm$ of the Θ^+. Comparing the

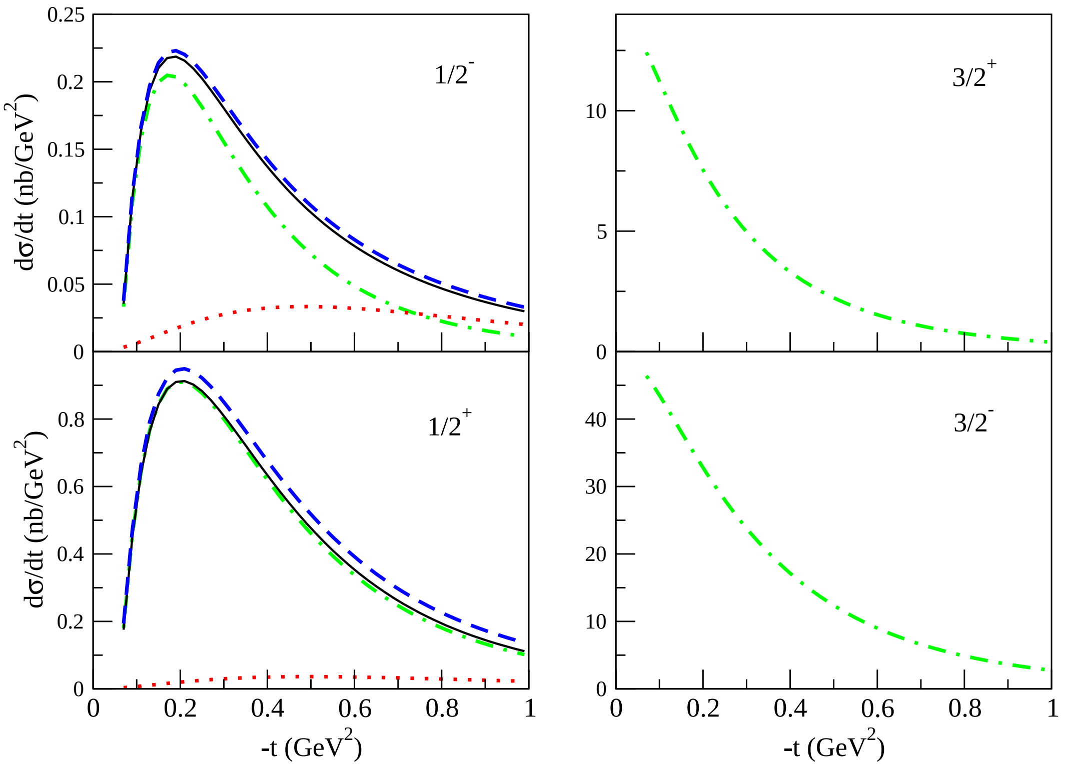

Figure 2: Regge model predictions for the $\gamma n \to K^- \Theta^+$ cross section at $E_\gamma = 4$ GeV for different spin parity assignments of the Θ^+. Dashed-dotted curves : gauge invariant K Regge exchange; dotted curves : K^* Regge exchange (for the cases of $1/2^\pm$). To account for the range of uncertainty in the $K^* N \Theta$ coupling, we display the result for $K + K^*$ exchange for two values of the $K^* N \Theta$ coupling constant : $f_{K^* N \Theta} = +1.1$ (solid curves), and $f_{K^* N \Theta} = -1.1$ (dashed curves), corresponding with a width $\Gamma_{\Theta \to K N} = 1$ MeV.

cross sections for K Regge exchange for the cases of $J^P = 1/2^\pm$, one notices that the $KN\Theta$ coupling constant for the case of a negative parity Θ^+ is a factor 7 smaller than for the case of a positive parity Θ^+. If there were only t-channel K exchange, this would result in a ratio of about a factor 50 for the cross sections of positive parity compared to negative parity Θ^+ photoproduction for the case of a Θ^+ of $J = 1/2$. The cross section for $J^P_\Theta = 1/2^-$ gets enhanced though through the u-channel Θ^+ process and the contact diagrams, which are required to make the t-channel charged kaon exchange process gauge-invariant. They are also responsible for the pronounced peak structure in the differential cross section at low values of $-t$. For the cases of $J^P_\Theta = 3/2^\pm$, the situation is reversed, as the $KN\Theta$ coupling constant is about a factor 7 larger for the case of $3/2^-$ compared with the case of $3/2^+$ when using a same width for the Θ^+. Taking into account the u-channel and contact diagrams then yields cross sections for the case of $3/2^-$ which are about a factor of 4 larger than for

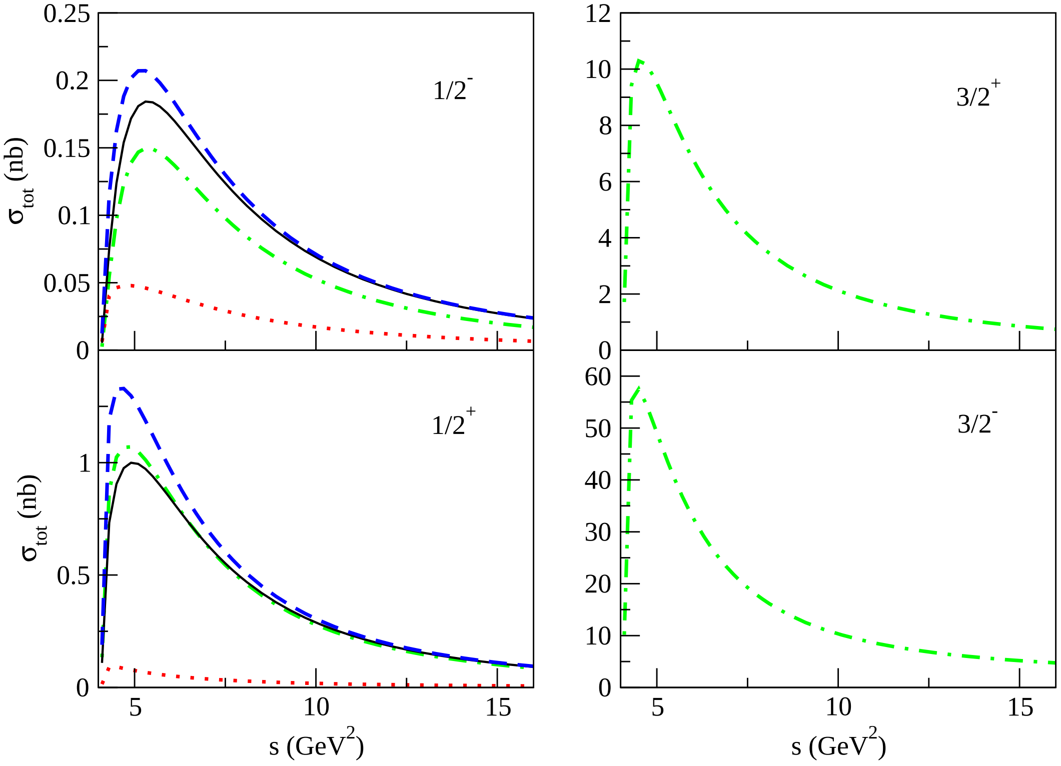

Figure 3: Regge model predictions for the $\gamma n \to K^- \Theta^+$ total cross sections for different spin-parity assignments of the Θ^+ resonance. Curve conventions as in Fig. 2.

the case of $3/2^+$.

In Fig. 2, we also show our estimates for the K^* exchange process for the spin-parity assignments $1/2^\pm$. To show the range of uncertainty arising from the $K^* N \Theta$ coupling, we display our results for two values : $f_{K^* N \Theta} = +1.1$ and $f_{K^* N \Theta} = -1.1$. The value $f_{K^* N \Theta} = +1.1$ is obtained by rescaling the chiral quark soliton model coupling for the case $J^P_\Theta = 1/2^+$ by the same amount as when rescaling the model value of $g_{K N \Theta}$ to correspond to a width of 1 MeV. One notices from Fig. 2 that for a $K^* N \Theta$ coupling within this range, the resulting K^* Regge exchange process yields only a very small contribution to the cross section compared with the gauge-invariant K exchange, in particular for the case of $1/2^+$. Furthermore, in the forward direction the K^* exchange process vanishes due to the momentum $(q - p_K)$ dependence in the $\gamma K K^*$ vertex. Such a behavior has been confirmed by data for the $\gamma p \to K^+ \Sigma^0$ reaction which is dominated by K^* exchange at large s and small $-t$, see Ref. [56]. Analogously, the forward angular region $(-t << s)$ for the $\gamma n \to K^- \Theta^+$ reaction at high photon energy is dominated by charged K exchange. At larger values of $-t$ the relative weight of K^* versus K exchange increases. Using the same values for the $K^* N \Theta$

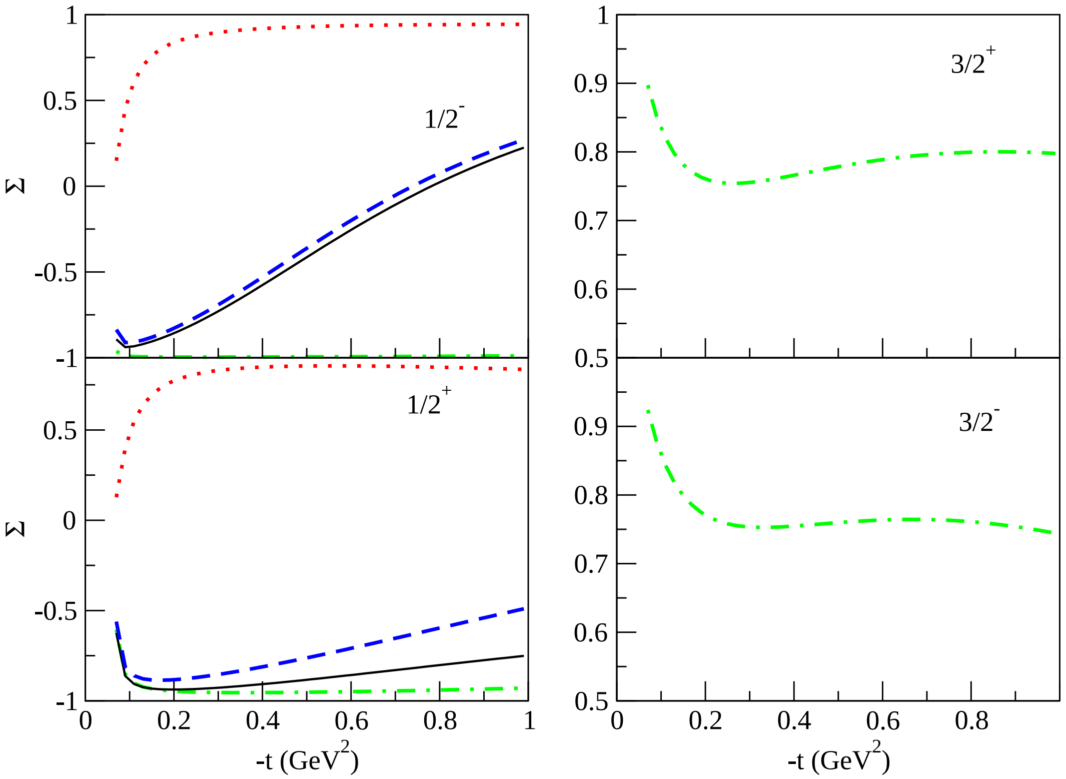

Figure 4: Regge model predictions for the $\gamma n \rightarrow K^- \Theta^+$ photon asymmetry at $E_\gamma = 4$ GeV for different spin parity assignments of the Θ^+. Curve conventions as in Fig. 2.

coupling in case $J^P_\Theta = 1/2^-$, the K^* exchange contribution becomes comparable to the gauge-invariant K exchange for values around $-t \simeq 1$ GeV^2.

In Fig. 3, we show the corresponding total cross sections. Using a width of 1 MeV for the Θ^+, the maximum value of the total cross sections can be seen to be around 1 nb for the case of $1/2^+$ and 0.2 nb for the case of $1/2^-$. For the cases of $3/2^+$ ($3/2^-$) much larger cross sections of around 10 nb (55 nb) are obtained when using a same value of 1 MeV for the Θ^+ width.

A direct measure of the relative weight of K versus K^* exchange processes can be obtained by the linear photon asymmetry, defined as :

$$\Sigma = \frac{\sigma_\perp - \sigma_\parallel}{\sigma_\perp + \sigma_\parallel}, \tag{29}$$

where $\sigma_\parallel$ and $\sigma_\perp$ are the cross sections induced by a linearly polarized photon beam with polarization vector lying in the reaction plane (for $\sigma_\parallel$) and perpendicular to the reaction plane (for $\sigma_\perp$) respectively. At high s and small $-t$ (with $-t << s$) the photon asymmetry for a natural parity t-channel exchange (such as for the K^*) approaches the value $+1$ (i.e. $\sigma_\perp$ dominates), whereas the photon asymmetry for an unnatural parity t-channel exchange process (such as for the K) yields the value -1 (i.e. $\sigma_\parallel$ dominates). The u-channel process and contact diagram, which are needed to make the t-channel K exchange gauge invariant are responsible for the deviation of the photon asymmetry from the value of -1, as is seen on Fig. 4. As the $\gamma n \to K^- \Theta^+$ process at large s and low $-t$ is dominated by K exchange, one sees from Fig. 4 that the photon asymmetry rises sharply, at small $-t$, to a large negative value for the cases of $1/2^\pm$. At larger values of $-t$ (for $-t \geq 0.2$ GeV^2), one sees from Fig. 4 that the influence of the K^* exchange in the photon asymmetry shows up, in particular for the case of $1/2^-$. The photon asymmetry seems therefore to be a very promising signature to distinguish between the $J^P_\Theta = 1/2^+$ and $J^P_\Theta = 1/2^-$ cases.

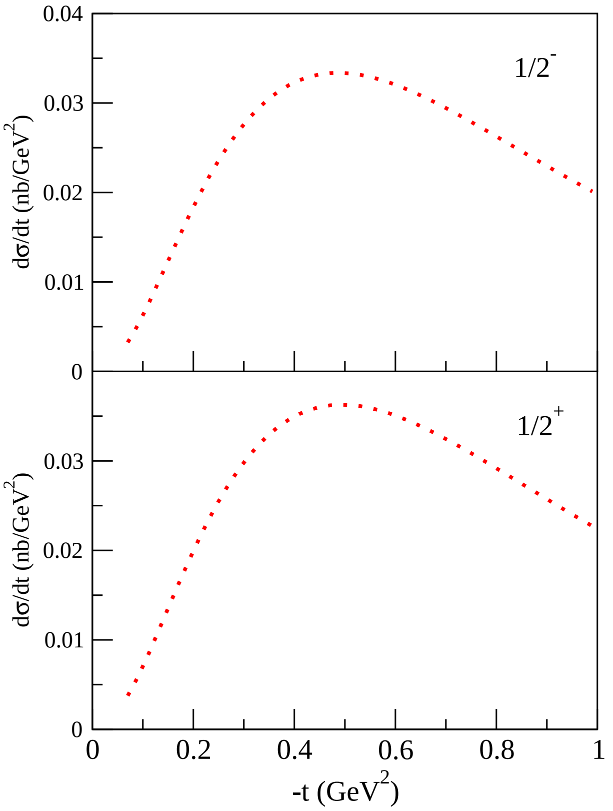

Figure 5: Regge model predictions for the $\gamma p \to \bar{K}^0 \Theta^+$ cross section at $E_\gamma = 4$ GeV for different spin-parity assignments of the Θ^+. Dotted curves : K^* Regge exchange.

In Fig. 5, we show the corresponding observables for the $\gamma p \to \bar{K}^0 \Theta^+$. For the neutral

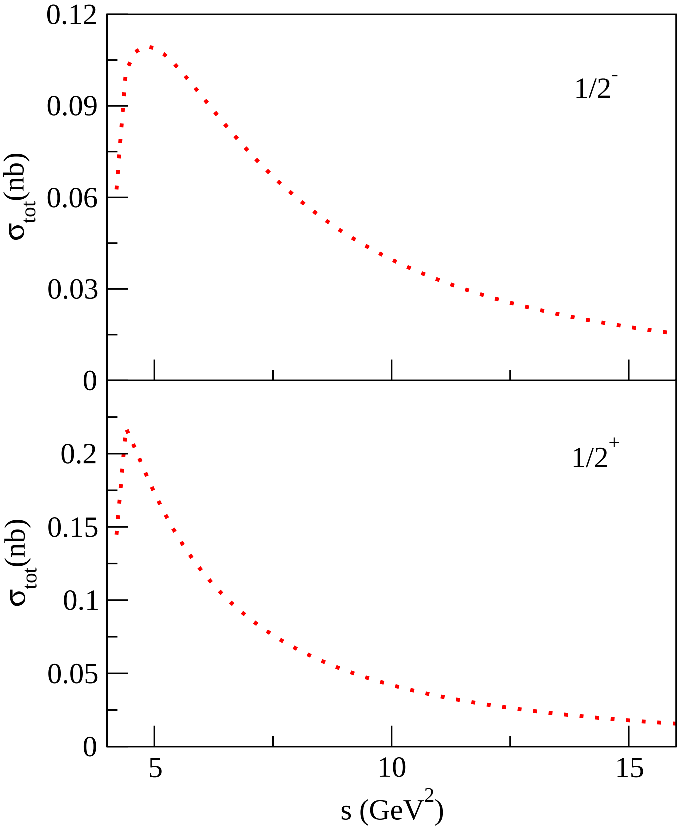

Figure 6: Regge model predictions for the $\gamma p \to \bar{K}^0 \Theta^+$ total cross sections for different spin-parity assignments of the Θ^+ resonance. Dotted curves : K^* Regge exchange.

kaon production reaction, the t-channel K exchange is absent, and the dominant t-channel mechanism is K^* exchange. One therefore sees from Figs. 5,7 that the observables carry the signatures of a K^* dominated process, i.e. a differential cross section which vanishes in the low t region and a photon asymmetry which reaches large positive values. By comparing the processes on the neutron (in Fig. 3) and on the proton (in Fig. 6), one notices that the absence of the K exchange mechanism yields cross sections on the proton that are about a factor 5 to 10 smaller than their counterparts on the neutron for the cases of $J^P_\Theta = 1/2^\pm$.

We next study the sensitivity of single target or recoil polarization observables for the $\gamma n \to K^- \Theta^+$ reaction, to the spin-parity assignments $J^P_\Theta = 1/2^+$ and $J^P_\Theta = 1/2^-$. The single target spin asymmetry (T) is defined as :

$$T = \frac{\sigma_\Uparrow - \sigma_\Downarrow}{\sigma_\Uparrow + \sigma_\Downarrow}, \tag{30}$$

where $\sigma_\Uparrow$ ($\sigma_\Downarrow$) are the cross sections where the target spin is polarized along (opposite) to

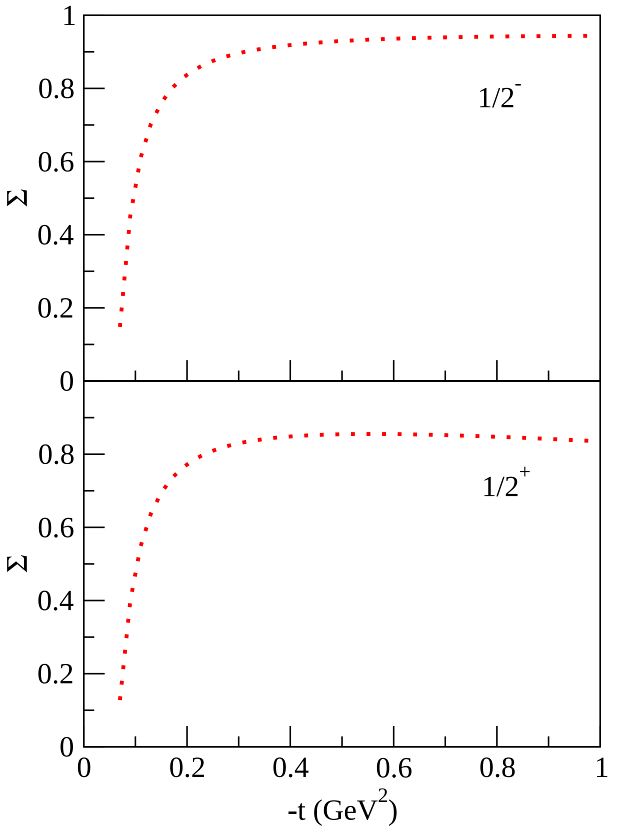

Figure 7: Regge model predictions for the $\gamma p \to \bar{K}^0 \Theta^+$ photon asymmetry at $E_\gamma = 4$ GeV for different spin-parity assignments of the Θ^+. Dotted curves : K^* Regge exchange.

the vector $\hat{n} \equiv (\vec{q} \times \vec{p}_K)/|\vec{q} \times \vec{p}_K|$, normal to the reaction plane. The recoil spin asymmetry (P) is defined in an analogous way, where the Θ^+ has its spin polarized along or opposite to the normal vector $\hat{n}$. In Figs. 8 and 9, we compare the Regge model results for T and P for both Θ^+ spin-parity assignments $1/2^{\pm}$. We first notice that the observables T and P are proportional to an imaginary part of the interference of two amplitudes. Therefore, one only obtains a non-zero value for T or P when the two interfering amplitudes exhibit a phase difference. The K exchange or the K^* exchange processes by themselves give us therefore a zero value for the asymmetries T and P. Their sum however leads to a non-zero value for T and P as shown in Figs. 8 and 9, due to the phase difference between the K and K^* Regge amplitudes. We see from Figs. 8 and 9 that for $J^P_\Theta = 1/2^+$, T and P have an opposite sign. On the other hand for the situation $J^P_\Theta = 1/2^-$, T and P display the same sign.

Besides the observables discussed above, where one integrates over all possible final states for the Θ^+ decay, one can also observe the decay angular distributions of the Θ^+. They show a characteristic dependence on the spin and parity of the final state. In the appendix, we

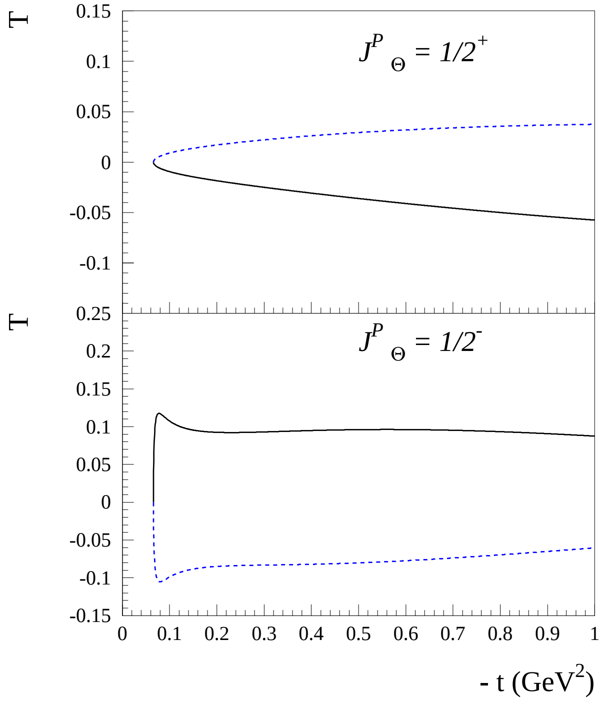

Figure 8: Regge model predictions for the target single spin asymmetry T for the $\gamma n \to K^- \Theta^+$ reaction for both possible parities of the Θ^+ resonance (for $J = 1/2$) at $E_\gamma = 4$ GeV. The model calculations correspond with the $K + K^*$ Regge exchanges for two values of the $K^* N \Theta$ coupling. Solid curves : $f_{K^* N \Theta} = +1.1$, dashed curves : $f_{K^* N \Theta} = -1.1$.

list the Θ^+ decay angular distributions for the spin-parity assignments $1/2^\pm$ and $3/2^\pm$.

We show the decay angular distributions for different photon polarizations : unpolarized (0) (Fig. 10), linearly polarized in the reaction plane (x) (Fig. 11), linearly polarized perpendicular to the reaction plane (y) (Fig. 12), and left-handed circular polarization (c, left) (Figs. 13 and 14). For the spin-parity assignments of $1/2^\pm$, one notices that the decay angular distributions (0), (x) and (y) display a nearly flat angular dependence. The decay angular distribution for a circularly polarized photon (c, left) on the other hand, is flat for the case of $1/2^-$ but not uniform for $1/2^+$, allowing to distinguish between both parity cases. All decay angular distributions show characteristic angular dependences in the case of $3/2^\pm$, which would be easily distinguishable from the $1/2^\pm$ case.

In Fig. 15, we also show our results for the $\gamma p \to \bar{K}^{*0} \Theta^+$ reaction. For this process, the dominant t-channel exchange mechanism, at high s and low $-t$, is given by K^0 exchange as shown in Fig. 1 (lower right panel). This yields to strong forwardly peaked angular

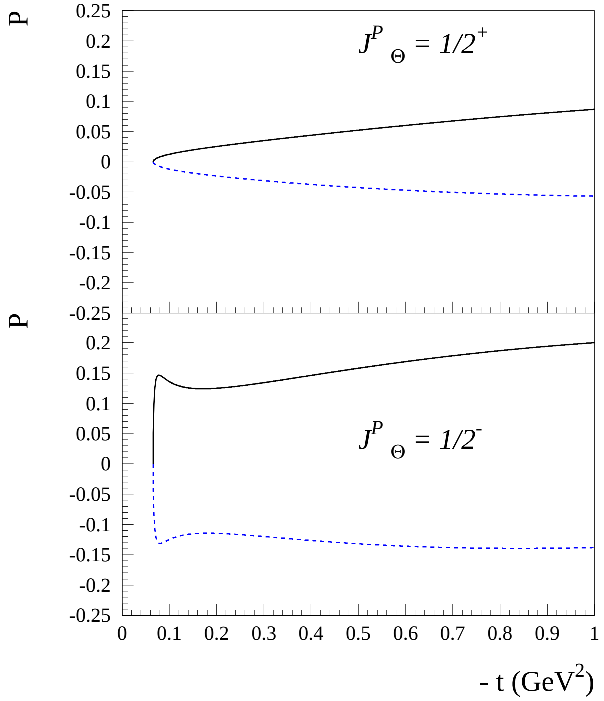

Figure 9: Regge model predictions for the recoil single spin asymmetry P for the $\gamma n \to K^- \Theta^+$ reaction for both possible parities of the Θ^+ resonance (for $J = 1/2$) at $E_\gamma = 4$ GeV. Curve conventions as in Fig. 8.

distributions, as is seen from Fig. 15. For a Θ^+ width of 1 MeV, the $1/2^+$ $(1/2^-)$ total cross sections reach a maximum value of 1.2 nb (0.2 nb) respectively.

IV. CONCLUSIONS

In this work, we studied the reaction mechanism for the photoproduction of the $\Theta^+(1540)$ resonance on the nucleon, through K and K^* Regge exchanges. Our estimates depend on only two parameters : the $KN\Theta^+$ and $K^*N\Theta^+$ coupling constants. The $KN\Theta^+$ coupling constant is directly related to the Θ^+ width. We determine the $K^*N\Theta^+$ coupling constant by rescaling the value obtained from the chiral quark soliton model by the same amount one has to rescale the $KN\Theta^+$ coupling to yield a given value of the Θ^+ width.

In the Regge model, which is assumed to be valid above *c.m.* energies above 2 GeV, the Θ^+ photoproduction cross sections show a strong forward angular dependence. We compared the size of the cross sections for the $\gamma n \to K^- \Theta^+$ and $\gamma p \to \bar{K}^0 \Theta^+$ reactions, and investigate

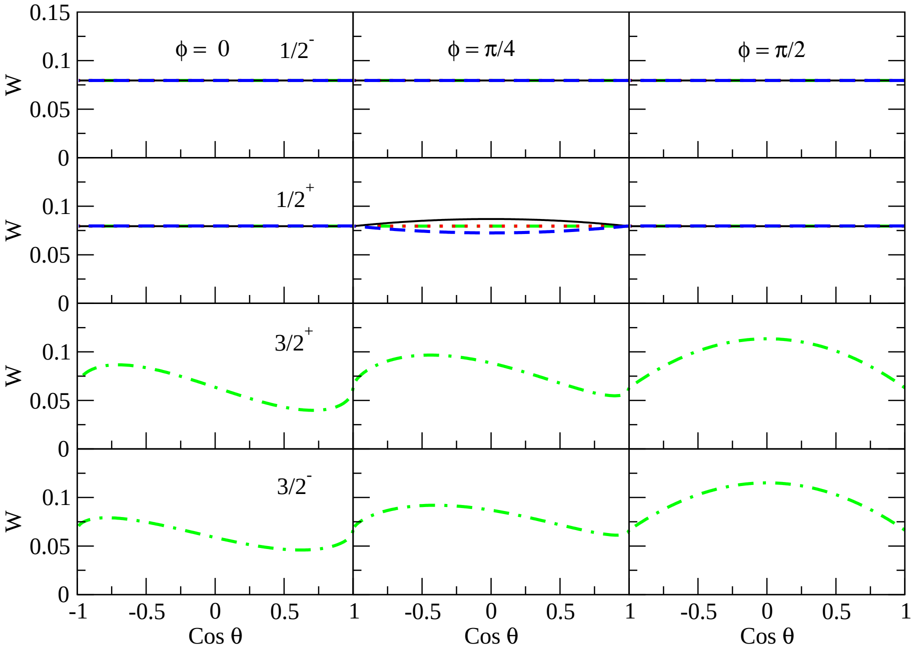

Figure 10: Regge model predictions for the $\gamma n \to K^- \Theta^+$ angular distribution for an unpolarized photon (0) for different spin parity assignments of the Θ^+, and for different decay angles (θ, ϕ), defined in the rest frame of the Θ^+. Dashed-dotted curves : K Regge exchange; dotted curves : K^* Regge exchange; solid curves : $K + K^*$ Regge exchanges.

their sensitivity to the spin-parity assignments $J^P = \frac{1}{2}^{\pm}, \frac{3}{2}^{\pm}$ for the Θ^+ resonance. Using the Regge model, we estimated the cross sections corresponding with a given upper bound on the width of the Θ^+. Within this model, the cross sections on the neutron were found to be around a factor 5 larger than the ones on the proton, due to the presence of charged K exchange for the reaction on a neutron target. For the case of spin-parity $J^P = \frac{1}{2}^+$, we found that a Θ^+ width of 1 MeV yields $\gamma n \to K^- \Theta^+$ cross sections of around 1 nb, and $\gamma p \to \bar{K}^0 \Theta^+$ cross sections around 0.2 nb. In the absence of a signal of the Θ^+ in such reactions, our estimates may be used to translate a given cross section upper limit into an upper bound on the width of the Θ^+.

Furthermore, we also estimated the photon asymmetry which was found to display a pronounced sensitivity to the parity of the Θ^+. Provided the Θ^+ can be produced, the photon asymmetry would be a very promising observable to help determining the quantum numbers of the Θ^+ resonance.

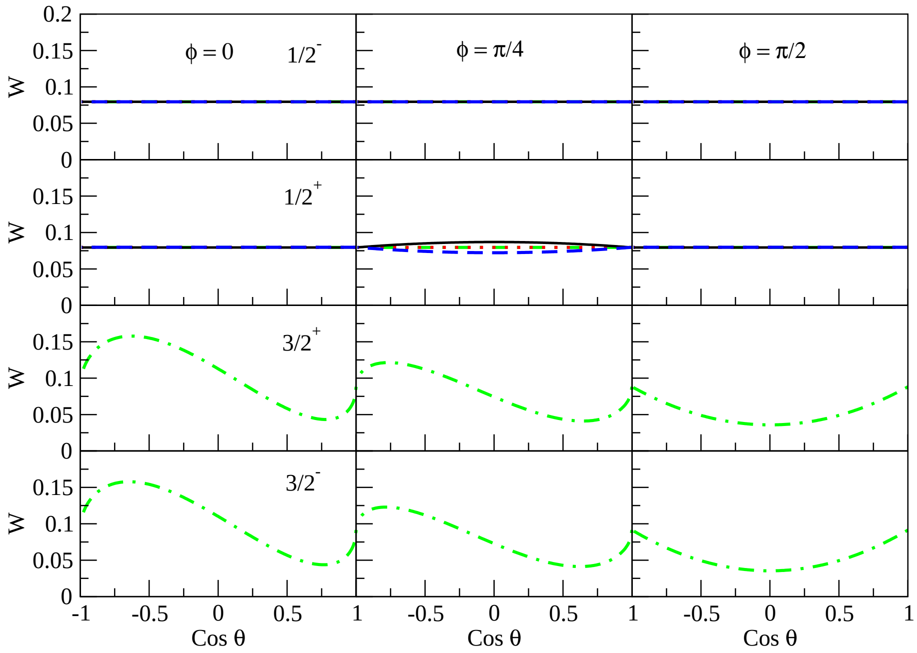

Figure 11: Regge model predictions for the $\gamma n \to K^-\Theta^+$ angular distribution for a photon linearly polarized in the reaction plane (x) for different spin parity assignments of the Θ^+. Curve conventions as in Fig. 10.

Acknowledgments

This work was supported by the U.S. Department of Energy under contract DE-AC05-84ER40150. H.J.K. is supported in part by the National Science Foundation under grant No. PHY-0456525 and by a SURA Fellowship. M.G. is supported by the French Centre National de la Recherche Scientifique. M.V.P. is supported by the Sofya Kovalevskaya Programme of the Alexader von Humboldt Foundation.

Appendix A: DECAY ANGULAR DISTRIBUTION

After produced, the Θ^+ decays into $\bar{K}^0 p$ or $K^+ n$ in 50% ratio. The angular distribution of the decay product (Kaon) can be determined by:

$$\begin{aligned} W(\theta,\phi) &= \sum_{s_f,s_f';s_\theta,s_\theta'} \hat{R}_{s_f,s_\theta}\rho_{s_\theta,s_\theta'}(\Theta^+)\hat{R}^*_{s_f',s_\theta'} \\ &= \sum_{s_\theta,s_\theta'} \{\hat{R}_{-\frac{1}{2},s_\theta}\rho_{s_\theta,s_\theta'}\hat{R}^*_{-\frac{1}{2},s_\theta'} + \hat{R}_{\frac{1}{2},s_\theta}\rho_{s_\theta,s_\theta'}\hat{R}^*_{-\frac{1}{2},s_\theta'} \\ &\quad + \hat{R}_{\frac{1}{2},s_\theta}\rho_{s_\theta,s_\theta'}\hat{R}^*_{\frac{1}{2},s_\theta'} + \hat{R}_{-\frac{1}{2},s_\theta}\rho_{s_\theta,s_\theta'}\hat{R}^*_{\frac{1}{2},s_\theta'}\}\,, \end{aligned} \tag{A1}$$

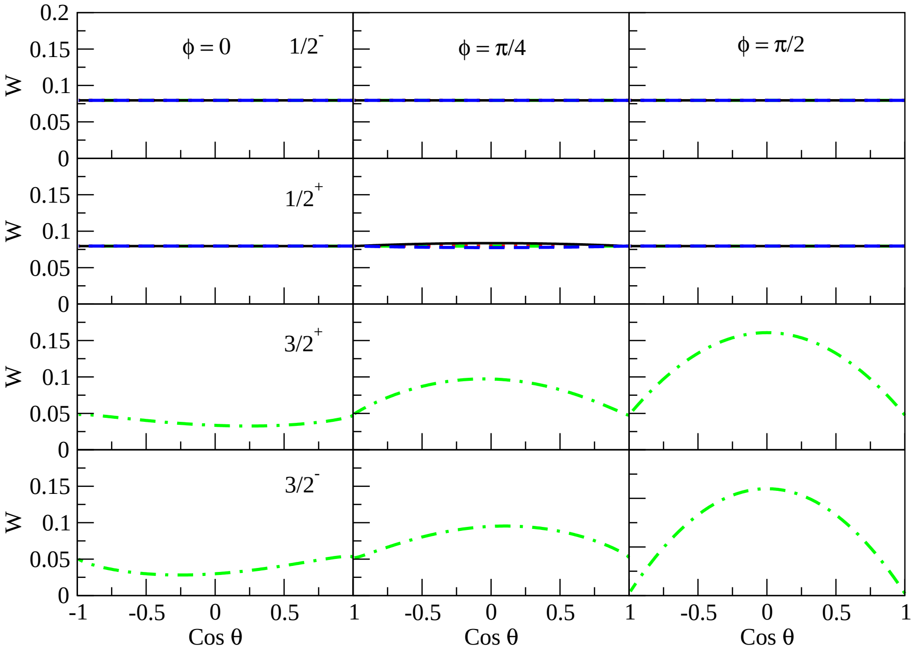

Figure 12: Regge model predictions for the $\gamma n \to K^-\Theta^+$ angular distribution for a photon linearly polarized perpendicular to the reaction plane (y) for different spin parity assignments of the Θ^+. Curve conventions as in Fig. 10.

where the transition operator $\hat{R}_{s_f,s_\theta}$ is defined as follow:

$$\hat{R}_{s_f,s_\theta} \equiv \langle N, s_f, \mathbf{P}_\theta - \mathbf{p}' | \hat{t} | \Theta^+, s_\theta, \mathbf{P}_\theta = 0 \rangle \,, \tag{A2}$$

and the photon density matrix elements $\rho_{s_\theta,s'_\theta}$ in the Θ^+ production can be obtained by squaring the amplitude $\mathcal{M}_K\,(\gamma N \to \Theta^+ K)$ of the corresponding spin of the Θ^+ and summing over the spin of the nucleon and the helicity of the photon.

The transition operator $\hat{R}_{s_f,s_\theta}$ depends on the spin of the particles involved. Below is the list of the transition operator $\hat{R}_{s_f,s_\theta}$ we use in this paper:

- $J^P = \frac{1}{2}^-$

$$\hat{R}_{s_f,s_\theta} = \mathcal{C}\delta_{s_f,s_\theta}$$

- $J^P = \frac{1}{2}^+$

$$\begin{aligned} \hat{R}_{\frac{1}{2},\frac{1}{2}} &= \cos\theta \\ \hat{R}_{\frac{1}{2},-\frac{1}{2}} &= -\sin\theta \; e^{-i\phi} \end{aligned}$$

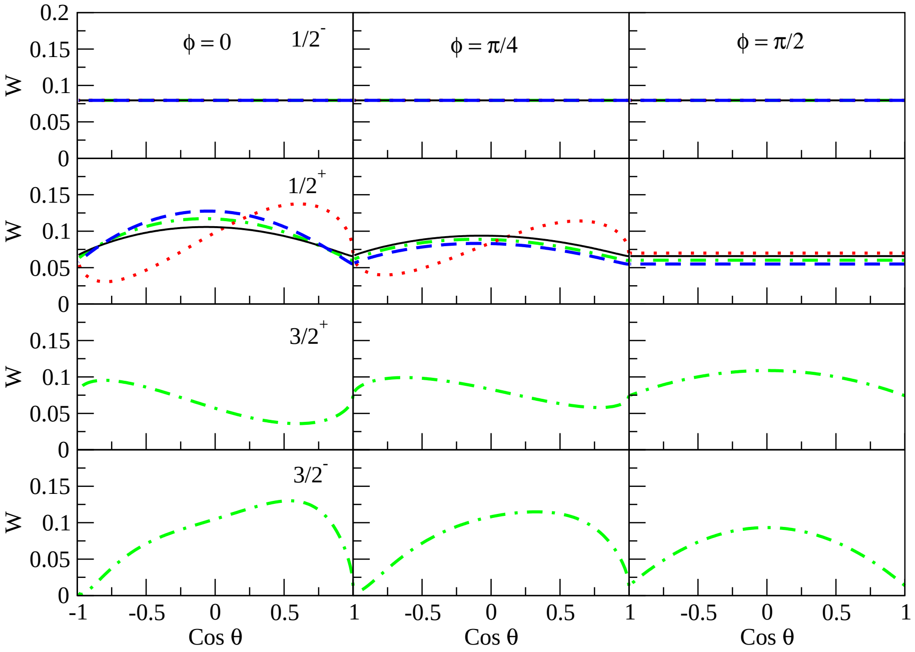

Figure 13: Regge model predictions for the $\gamma n \to K^- \Theta^+$ angular distribution for a left-handed circularly polarized photon (c, left) for different spin parity assignments of the Θ^+. Curve conventions as in Fig. 10.

$$\hat{R}_{-\frac{1}{2},\frac{1}{2}} = -\sin\theta \; e^{i\phi}$$

$$\hat{R}_{-\frac{1}{2},-\frac{1}{2}} = -\cos\theta$$

- $J^P = \frac{3}{2}^+$

$$\hat{R}_{\frac{1}{2},\frac{3}{2}} = \frac{\sin\theta}{\sqrt{2}} \; e^{i\phi}$$

$$\hat{R}_{\frac{1}{2},\frac{1}{2}} = \sqrt{\frac{2}{3}}\cos\theta$$

$$\hat{R}_{\frac{1}{2},-\frac{1}{2}} = -\sqrt{\frac{1}{6}}\sin\theta \; e^{-i\phi}$$

$$\hat{R}_{-\frac{1}{2},\frac{1}{2}} = \sqrt{\frac{1}{6}}\sin\theta \; e^{i\phi}$$

$$\hat{R}_{-\frac{1}{2},-\frac{1}{2}} = \sqrt{\frac{2}{3}}\cos\theta$$

$$\hat{R}_{-\frac{1}{2},-\frac{3}{2}} = -\frac{\sin\theta}{\sqrt{2}} \; e^{i\phi}$$

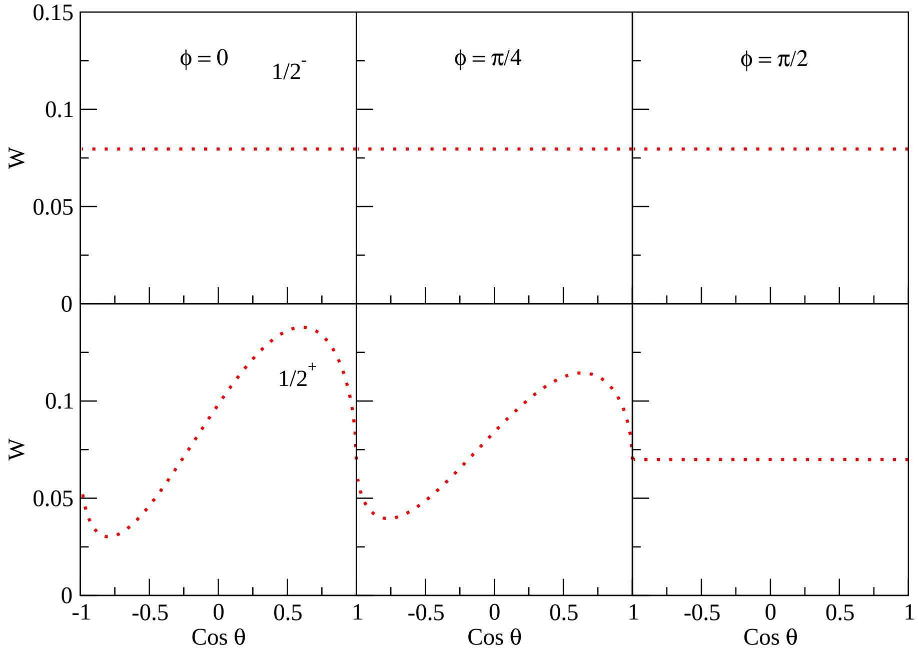

Figure 14: Regge model predictions for the $\gamma p \to K^0\Theta^+$ angular distribution (c, left) for different spin parity assignments of the Θ^+. Dotted curves : K^* Regge exchange.

- $J^P = \frac{3}{2}^-$

$$
\begin{aligned}
\hat{R}_{\frac{1}{2},\frac{3}{2}} &= -\sqrt{\frac{3}{40}}\sin 2\theta\ e^{i\phi} \\
\hat{R}_{\frac{1}{2},\frac{1}{2}} &= -\sqrt{\frac{1}{10}}(3\cos^2\theta - 1) \\
\hat{R}_{\frac{1}{2},-\frac{1}{2}} &= \sqrt{\frac{9}{40}}\sin 2\theta\ e^{-i\phi} \\
\hat{R}_{\frac{1}{2},-\frac{3}{2}} &= -\sqrt{\frac{3}{10}}\sin^2\theta\ e^{-2i\phi} \\
\hat{R}_{-\frac{1}{2},\frac{3}{2}} &= \sqrt{\frac{3}{10}}\sin^2\theta\ e^{2i\phi} \\
\hat{R}_{-\frac{1}{2},\frac{1}{2}} &= \sqrt{\frac{9}{40}}\sin 2\theta\ e^{i\phi} \\
\hat{R}_{-\frac{1}{2},-\frac{1}{2}} &= \sqrt{\frac{1}{10}}(3\cos^2\theta - 1) \\
\hat{R}_{-\frac{1}{2},-\frac{3}{2}} &= -\sqrt{\frac{3}{40}}\sin 2\theta\ e^{-i\phi}
\end{aligned}
$$

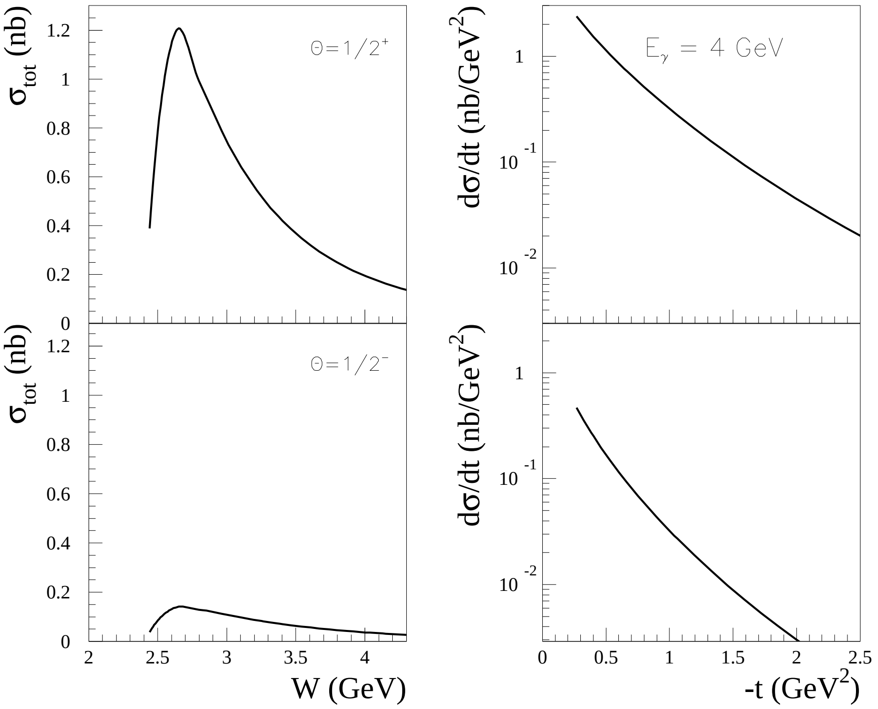

Figure 15: Regge model predictions for the $\gamma p \to \bar{K}^{*0}\Theta^+$ reaction for both possible parities of the Θ^+ resonance. Upper panels : positive parity case; lower panels : negative parity case. Left panels : total cross section; right panels : differential cross section at $E_\gamma = 4$ GeV. The model calculation corresponds with K^0 Regge exchange.

[1] T. Nakano *et al.* (LEPS Collaboration), Phys. Rev. Lett. **91**, 012002 (2003).

[2] V. Barmin *et al.* (DIANA Collaboration), Phys. Atom. Nucl. **66**, 1715 (2003) [Yad. Fiz. **66**, 1763 (2003)].

[3] S. Stepanyan *et al.* (CLAS Collaboration), Phys. Rev. Lett. **91**, 252001 (2003).

[4] J. Barth *et al.* (SAPHIR Collaboration), Phys. Lett. B **572**, 127 (2003).

[5] V. Kubarovsky *et al.* (CLAS Collaboration), Phys. Rev. Lett. **92**, 032001 (2004) [Erratum-ibid. **92**, 049902 (2004)].

[6] A. Airapetian *et al.* (HERMES Collaboration), Phys. Lett. B **585**, 213 (2004).

[7] A. E. Asratyan, A. G. Dolgolenko and M. A. Kubantsev, Phys. Atom. Nucl. **67**, 682 (2004)

[Yad. Fiz. **67**, 704 (2004)] [arXiv:hep-ex/0309042].

[8] A. Aleev *et al.* [SVD Collaboration], arXiv:hep-ex/0401024.

[9] M. Abdel-Bary *et al.* (COSY-TOF Collaboration), Phys. Lett. B **595**, 127 (2004).

[10] S. Chekanov *et al.* [ZEUS Collaboration], Phys. Lett. B **591**, 7 (2004) [arXiv:hep-ex/0403051].

[11] C. Alt *et al.* [NA49 Collaboration], Phys. Rev. Lett. **92**, 042003 (2004) [arXiv:hep-ex/0310014].

[12] J. Z. Bai *et al.* [BES Collaboration], Phys. Rev. D **70**, 012004 (2004) [arXiv:hep-ex/0402012].

[13] B. Aubert *et al.* [BABAR Collaboration], arXiv:hep-ex/0408064.

[14] K. Abe *et al.* [BELLE Collaboration], arXiv:hep-ex/0409010.

[15] S. R. Armstrong, Nucl. Phys. Proc. Suppl. **142**, 364 (2005) [arXiv:hep-ex/0410080]; S. Schael *et al.* [ALEPH Collaboration], Phys. Lett. B **599**, 1 (2004).

[16] I. Abt *et al.* [HERA-B Collaboration], Phys. Rev. Lett. **93**, 212003 (2004).

[17] Y. M. Antipov *et al.* [SPHINX Collaboration], Eur. Phys. J. A **21**, 455 (2004).

[18] M. J. Longo *et al.* [HyperCP Collaboration], Phys. Rev. D **70**, 111101 (2004).

[19] D. O. Litvintsev [CDF Collaboration], Nucl. Phys. Proc. Suppl. **142**, 374 (2005).

[20] K. Stenson [FOCUS Collaboration], arXiv:hep-ex/0412021.

[21] K. Abe *et al.* [Belle Collaboration], arXiv:hep-ex/0411005.

[22] C. Pinkenburg [PHENIX Collaboration], J. Phys. G **30**, S1201 (2004).

[23] H. G. Fischer and S. Wenig, Eur. Phys. J. C **37**, 133 (2004) [arXiv:hep-ex/0401014].

[24] M. I. Adamovich *et al.* [WA89 Collaboration], Phys. Rev. C **70**, 022201 (2004); arXiv:hep-ex/0405042.

[25] K. H. Hicks, arXiv:hep-ex/0504027.

[26] "Review Of Particle Properties. Particle Data Group," Phys. Lett. B **170**, 1 (1986); Phys. Lett. B **204**, 1 (1988).

[27] D. Diakonov, V. Petrov, M. Polyakov, Z. Phys. A **359**, 305 (1997).

[28] H. Weigel, Eur. Phys. J. A **2**, 391 (1998).

[29] T. D. Cohen, Phys. Lett. B **581**, 175 (2004) [arXiv:hep-ph/0309111].

[30] H. Walliser and V. B. Kopeliovich, J. Exp. Theor. Phys. **97**, 433 (2003) [Zh. Eksp. Teor. Fiz. **124**, 483 (2003)] [arXiv:hep-ph/0304058].

[31] A. Hosaka, Phys. Lett. B **571**, 55 (2003).

[32] D. Borisyuk, M. Faber and A. Kobushkin, arXiv:hep-ph/0307370.

[33] M. Praszalowicz, Phys. Lett. B **575**, 234 (2003) [arXiv:hep-ph/0308114].

[34] C. E. Carlson, C. D. Carone, H. J. Kwee and V. Nazaryan, Phys. Lett. B **573**, 101 (2003).

[35] R.L. Jaffe, F. Wilczek, Phys. Rev. Lett. **91**, 232003 (2003).

[36] C.E. Carlson, C.D. Carone, H.J. Kwee, V. Nazaryan, Phys. Lett. B **579**, 52 (2004).

[37] Fl. Stancu, D.O. Riska, Phys. Lett. B **575**, 242 (2003).

[38] J. J. Dudek and F. E. Close, Phys. Lett. B **583**, 278 (2004) [arXiv:hep-ph/0311258].

[39] C. E. Carlson, C. D. Carone, H. J. Kwee and V. Nazaryan, Phys. Rev. D **70**, 037501 (2004).

[40] S. Capstick, P. R. Page and W. Roberts, Phys. Lett. B **570**, 185 (2003) [arXiv:hep-ph/0307019].

[41] B. K. Jennings and K. Maltman, Phys. Rev. D **69**, 094020 (2004) [arXiv:hep-ph/0308286].

[42] W. Liu, C. M. Ko, Phys. Rev. C **68**, 045203 (2003); nucl-th/0309023.

[43] S. I. Nam, A. Hosaka and H. C. Kim, Phys. Lett. B **579**, 43 (2004); Phys. Rev. D **70**, 114027 (2004); hep-ph/0403009.

[44] Y. Oh, H. Kim, S.H. Lee, Phys. Rev. D **69**, 014009 (2004).

[45] Q. Zhao, Phys. Rev. D **69**, 053009 (2004).

[46] K. Nakayama, K. Tsushima, Phys. Lett. B **583**, 269 (2004).

[47] Q. Zhao and J. S. Al-Khalili, Phys. Lett. B **585**, 91 (2004) [Erratum-ibid. B **596**, 317 (2004)].

[48] F. E. Close and Q. Zhao, Phys. Lett. B **590**, 176 (2004).

[49] K. Nakayama and W. G. Love, Phys. Rev. C **70**, 012201 (2004) [arXiv:hep-ph/0404011].

[50] T. Mart, Phys. Rev. C **71**, 022202 (2005) [arXiv:nucl-th/0412096].

[51] W. Roberts, Phys. Rev. C **70**, 065201 (2004) [arXiv:nucl-th/0408034]; arXiv:nucl-th/0412041.

[52] M. Diehl, B. Pire and L. Szymanowski, Phys. Lett. B **584**, 58 (2004) [arXiv:hep-ph/0312125].

[53] JLab Hall B experiment E-03-113, spokespersons K. Hicks et al.

[54] JLab Hall B experiment E-04-017, spokespersons M. Battaglieri, V. Kubarovsky, J. Price, D. Weygand.

[55] JLab Hall A experiment E-04-012, spokespersons B. Wojtsekhowski et al.

[56] M. Guidal, J.-M. Laget, and M. Vanderhaeghen, Nucl. Phys. A 627, 645 (1997).

[57] M. Guidal, J.-M. Laget, and M. Vanderhaeghen, Phys. Rev. C **61**, 025204 (2000); Phys. Rev. C **68**, 058201 (2003).

[58] N. Levy, W. Majerotto, and B. J. Read, Nucl.Phys. **55**, 493 (1973).

[59] P.D.B. Collins, *An Introduction to Regge Theory and High-Energy Physics* (Cambridge University Press, Cambridge, 1977).

[60] R. N. Cahn and G. H. Trilling, Phys. Rev. D **69**, 011501 (2004) [arXiv:hep-ph/0311245].

[61] L.M. Jones, Rev. Mod. Phys. **52**, 545 (1980).

[62] O. Dumbrajs, R. Koch, H. Pilkuhn, G. Oades, H. Behrens, J.J. de Swart, and P. Kroll, Nucl. Phys. **B 216** (1983) 277.

[63] G. Hoehler, F. Kaiser, R. Koch and E. Pietarinen, “Handbook of Pion-Nucleon Scattering”.